A DISCUSSION OF THE WATER CONTENT OF VERMICULITE

by

W. F. BRADLEY AND J. M. SERRATOSA[1]

Illinois Geological Survey, Urbana, Illinois

ABSTRACT

Selected chemical and diffraction analyses from the literature, supplemented by thermal and thermogravimetric analyses and infrared absorption observations, are utilized to construct a rational model of the water arrangement in natural vermiculites.

A super cell is arranged by simple modification of the Hendricks water nets to accommodate the somewhat higher water contents, indicated by weight loss analyses, and the exchangeable cations.

A three-cell unit (15.6 × 9 Å) contains two $Mg^{2+} \cdot 6H_2O$ octahedra centered at the corners and face centers and four $4H_2O$ squares centered about ± 5.2 Å along a between the octahedra. The arrangement affords twenty hydrogen bonds near 2.75 Å, twelve between silicate and water layers and eight between water layers, and thirty-two hydrogen bonds near 3.0 Å within water layers. The remaining four hydrogens are not active in the bonding system. The environment of each water molecule is a distorted tetrahedron.

A broad infrared absorption band shows maxima at about 3600, 3450 and 3350 cm^{-1} at normal incidence, with increased activity in the highest and lowest energies when a flake is tilted. It is concluded that OH axes in the shortest bonds are more inclined to the cleavage planes than are the intermediate length axes.

The essential geometrical features of the vermiculite structure were established by Hendricks and Jefferson (1938) and the activity of vermiculite in exchange processes was delineated by Barshad (1948). Subsequent analyses, including some substantial refinements (Mathieson and Walker, 1954; Grudemo, 1954), have substantially confirmed earlier interpretations but have led to varied inferences with regard to details of the disposition of the hydration water.

Atomic weight summations for the contents of a 9.2 × 5.3 × 14.4 Å cell are of the order of 1000, which in itself puts some burden upon the accuracy of a chemical analysis if it is to be reduced to an empirical formula, and in no case can such a reduction be made without allowance for the seldom determined exchangeable bases. Other features difficult to handle in the rationalization of any given analysis include the oxidating state of the iron content and the extent to which extraneous mica or chlorite layers intervene within the crystals analyzed.

Bases selected by different individuals for rationalization of chemical analysis vary in details, but have met an aggregate degree of success which encourages speculation. One reasonable presumption is that the frequency

[1] Permanent address: Instituto de Edafologia, CSIC, Madrid.

with which vermiculite is observed to be an alteration product of a biotite mica should lead to a significant number of instances in which the layer charge of a vermiculite closely corresponds to the common layer charge of micas. This thought has been appraised critically by Weaver (1958) and has been found by him to afford a valid parameter for the characterization of an extensive suite of vermiculite specimens. A second is that the higher oxidation state of iron frequently found in vermiculites was achieved after the layer charge was established in the parent mica composition. Laboratory oxidation experiments (as Brindley and Youell, 1953) indicate that ferrous iron in the hydrous layer silicates undergoes oxidation with concomitant loss of protons from hydroxyl ions, thus retaining the original layer charge.

The magnitudes of exchange capacities (which are measures of layer charge) are subject to moderate latitudes because of ease of exchange. They vary with the identity of the exchanging ion, and suffer from marked inhibition with increasing grain size. Pertinent, careful study of several vermiculites by Barshad (1948) established that ammonium acetate measured exchangeable Mg but not exchangeable K in convenient laboratory time, but that by exchanging K with $MgCl_2$ and then determining the capacity for Mg exchange by NH_4, augmented capacities, probably more commensurate with the layer charge, were observed.

The result is that quoted determined exchange capacities for vermiculites probably range from lower than to equal to, but not higher than, the layer charge. Also, ferric iron-bearing compositions probably are deficient in hydroxyl ions, so that derived empirical formulas frequently include a low estimate for molecular water.

Four reductions of analyses to empirical formulas are tabulated in Table 1. Each is arrived at by assumptions that the oxygen content per cell on ignited basis is equal to $22 + \frac{1}{2}$ the number of ferric iron ions, and that fourteen cations occupy the fourteen positions in the structural scheme, with any excess being taken as interlayer. Within the validity of the assumptions, this method appraises layer charge without regard to interlayer matter (or identity of intergrown layers). Sufficient hydroxyls (or fluoride) are then allocated to increase the O + OH (and F) occupancy to twenty-four, and additional water is assumed to be molecular. No one of the analyses is complete in all pertinent details, but the close correlation between the implications of the analysis of the iron-free specimen with those of the ferric iron-bearing materials constitutes fair evidence for the validity of the assumptions above. In the tabulation, layer charges are a net difference between tetrahedral deficiency and octahedral excess, and are approximately compensated by either or both of the calculated and determined interlayer ion entries.

The Grudemo and the Mathieson and Walker analyses relate to crystals on which they analyzed diffraction data, and Gruner's average is for analyses only of crystals he had inspected by diffraction methods. Supplemental information on the Llano crystals is cited here. Atom proportions are calculated from a wet analysis by Eileen H. Ozlund, and the Mg^{2+} exchange

TABLE 1.—ION POPULATIONS OF SOME VERMICULITES

Ion	Gruner's[1] Average Analysis	Grudemo's[2] Crystal C	Mathieson and Walker[3] from Kenya	White Crystal[4] from Llano, Texas
Si	5.84	5.66	5.56	5.68
Al_T	2.16	2.34	2.44	2.32
Al_O	0.50	0.84	0.50	0.25
Fe^{3+}	0.53	0.89	0.98	—
Ti^{4+}	—	—	—	0.03
Fe^{2+}	—	0.21	—	0.03
Mg	4.97	4.06	4.52	5.69
Mg^{2+}	0.87	0.74	0.96	0.90
Other bases^{2+}	—	—	—	0.08
Detnd. Exchange	None Detnd.	Capacity = 0.75[5]	Mg^{2+} = 0.64	Mg^{2+} = 0.875 (diffraction estimate ca. 90% complete)[6]
O	20.53	20.89	20.98	20.0
OH	3.47	3.11	3.02	3.74
F	—	—	—	0.26
H_2O	8.86	10.2	9.1	9.45 (analysis) 10.2 (thermogravimetric record)

[1] Gruner (1934).
[2] Grudemo (1954).
[3] Mathieson and Walker (1954).
[4] Analysis of Eileen H. Ozlund, Rock Analysis Laboratory, Univ. of Minn., furnished by S. E. Clabaugh.
[5] Barshad's citation from same occurrence.
[6] Introduction of Na^+ by exchange reduces layer thicknesses to about 11.8 Å, permitting observation of resolved diffraction effects from both reacted and unreacted material.

entry is Mg recovered by M NaCl leaching at room temperature of an unground crystal, inspected before and after by x-ray diffraction.

An equilibrium thermobalance weight loss curve and a conventional differential thermal analysis curve (Fig. 1) indicate overall water loss only a little greater than the chemical analysis, and consistent with the equivalent determination by Barshad on the sample that was also analyzed by Grudemo. The loss is seen to be partitioned into two major low-temperature categories and one major high-temperature category. An additional indistinct high-temperature feature around 600°C is presumed to indicate some loss of fluoride.

The water losses, as determined, and the water contents per cell derived

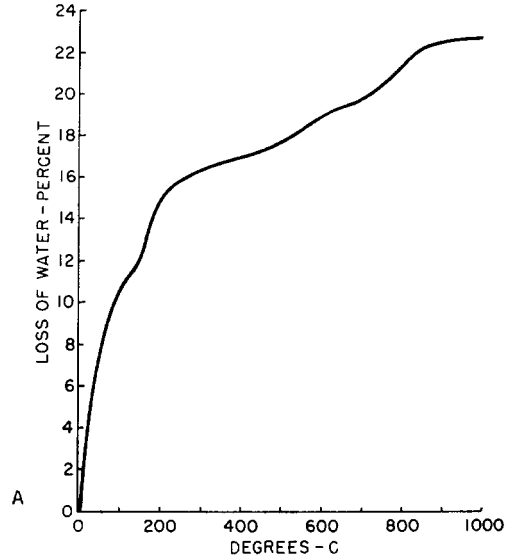

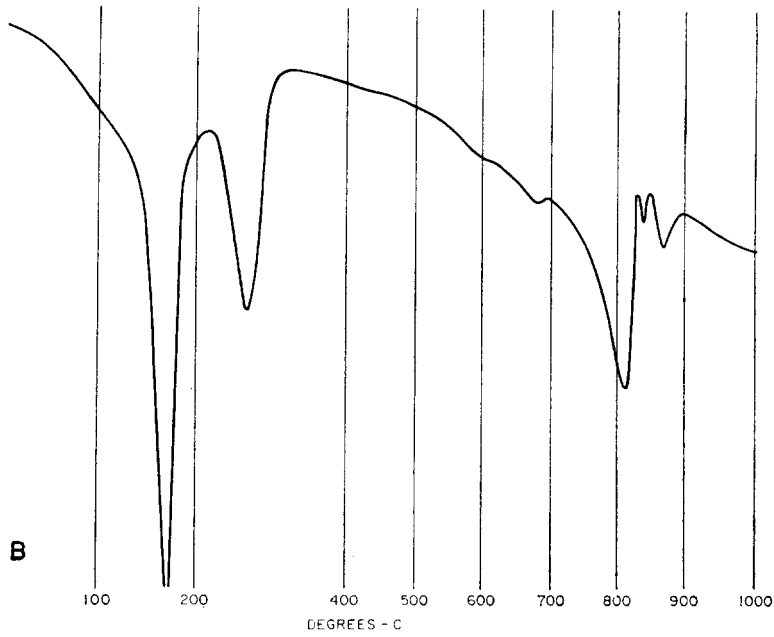

Figure 1.—(a) Thermobalance equilibrium weight loss curve, and (b) differential thermal analysis record for white vermiculite from Llano, Texas.

https://doi.org/10.1346/CCMN.1958.0070116 Published online by Cambridge University Press

from them run consistently above the 8 mole proportion that we used for calculating signs for a one-dimensional Fourier analysis of diffraction intensities from the same crystal when examining glycol complexes (Bradley *et al.*, 1958). Allocation of this additional water to the model reverses the calculated sign for the second order, so this corrected one-dimensional synthesis is reproduced in Fig. 2. In Fig. 2 the levels of z-parameters are marked, with compositions noted, and relative planimeter areas under the curve for those features which could be imagined resolved are scaled to electron units for the model.

Infrared absorption has been found to be highly useful in establishing the

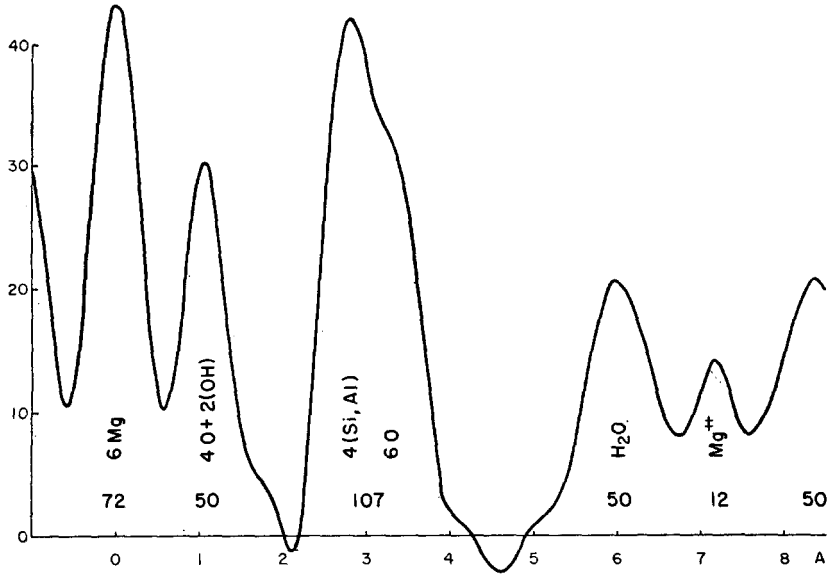

FIGURE 2.—One-dimensional Fourier synthesis from 00l diffraction intensities of the Llano, Texas, vermiculite. Coefficients were listed by Bradley *et al.* (1958), but in this present synthesis the sign of the second term is reversed. The numbers listed near each z-level are relative planimeter areas between the curve and the base line shown, and are to be compared with the pertinent sums of atomic numbers.

orientation of OH bonds in hydroxyls in the absence of molecular water (Serratosa and Bradley, 1958). Thinly cleaved Llano vermiculite was examined after moderate ignitions at normal and inclined incidence (Fig. 3) to confirm that the OH content exists in the polar orientation typical of trioctahedral compositions.

The infrared absorption character of hydration water in solids is less well established, and is more difficult to observe. No cleavage flakes of true vermiculite were found sufficiently thin so that resolution in the water frequencies at the natural water content levels could be observed. A hydrobiotite was therefore examined, the hydrobiotite being in effect vermiculite diluted with biotite, diffraction effects for which are illustrated in Fig. 4.

https://doi.org/10.1346/CCMN.1958.0070116 Published online by Cambridge University Press

Absorption curves shown in Fig. 5 indicate three poorly resolved bands near 3700 cm^{-1}, all less energetic than the free OH frequency. This particular hydrobiotite is highly colored and lacks any clearly resolved free OH feature. This could be due either to iron oxidation or to some fluoride content. Chemical analysis is not available, but diffraction character is typical, and the cleavage flakes were thin enough to permit view of the water absorption features modified but little by the 3700 cm^{-1} free OH absorption.

The theoretic grounds for infrared absorption by water of crystallization do not seem to have been developed. A starting point has been the allocation

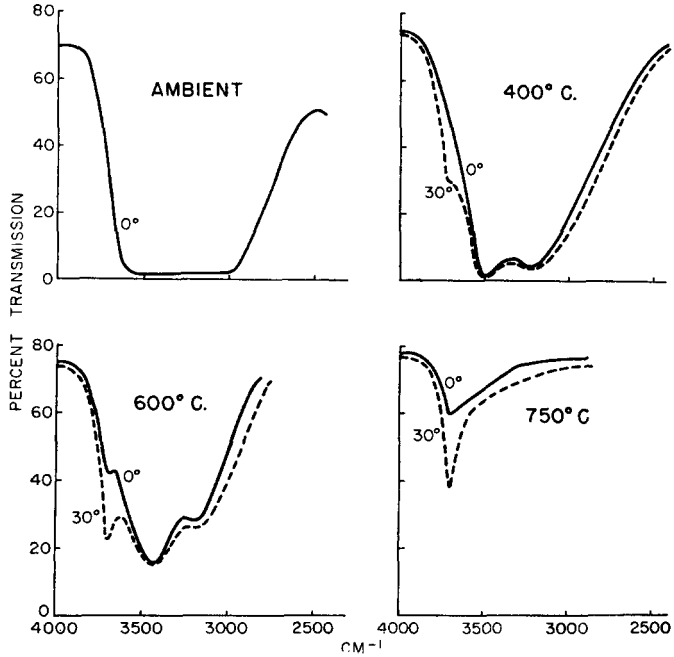

Figure 3.—Infrared absorption spectra of Llano vermiculite after heating to indicated temperatures, protecting the ignited flakes with Nujol. Full lines represent the spectra when light is incident along the normal to the flake, and dashed lines when it is incident at 30° to the normal. The features at about 3700 cm^{-1} arise from OH groups with axes normal to the flakes, and lower frequency features are from reabsorbed water, not completely excluded by the Nujol.

of one band in this region to unresolved symmetrical and antisymmetrical stretching frequencies. It would seem that these modes could be active only if both protons were equally bound within their own molecule. Hydrogen bonding is frequently inferred to modify bonding energies of protons to their oxygen nuclei one at a time. Unequal hydrogen bond lengths therefore are presumed to absorb independently at hydroxyl frequencies characteristic of the strength of the bond. In the vermiculite absorption feature we think we find, in order, absorption by a practically free O—H bond at about

https://doi.org/10.1346/CCMN.1958.0070116 Published online by Cambridge University Press

3600 cm^{-1}, the water stretching frequencies at about 3450 cm^{-1}, and stretching from short O—H · · · · O hydrogen bonds at about 3350 cm^{-1}. Below the hydrobiotite features in Fig. 5 are plotted the ratios of logs of reciprocals of transmission for the inclined incidence to those of the normal incidence curves illustrated. These imply that the highest and lowest frequencies both relate to OH bond axes significantly inclined to the plane of the cleavage flake. The intermediate ratio has essentially the value of the

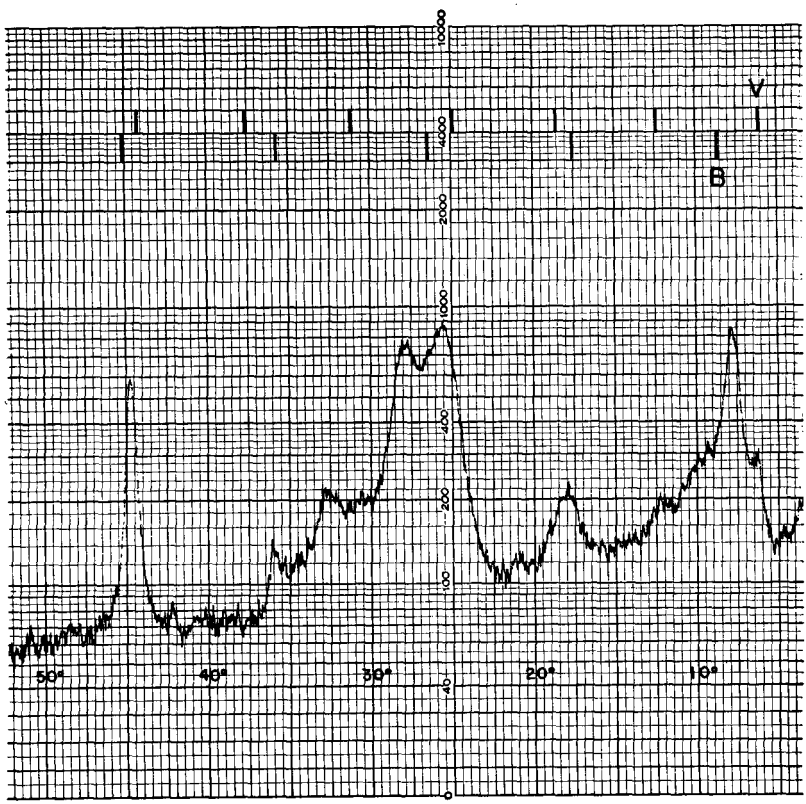

FIGURE 4.—Diffractometer record of the diffuse scattering along the 00*l* pole from the hydrobiotite cleavage flake. The position of nodes for biotite and for vermiculite are noted. (Filtered Cu radiation.)

path length ratios for an estimated angle of refraction (about 20°) and indicate OH bond axes near the plane of the flake.

The several lines of evidence can be reduced to a concensus that vermiculite consists of the standard talc layer and a double water layer disposed in about 80 percent of the positions occupied by " brucite " hydroxyls in the chlorite structures coordinated about exchangeable Mg^{2+} ions disposed in about 10–15 percent of the " brucite " magnesium positions in the chlorites. The latitudes demonstrate that less than crystalline regularity obtains in any

given case but an illustrative average case can be depicted. This was, in fact, done by Mathieson and Walker (1954) but directed toward a lower water content. In Fig. 6 the objective has been to accommodate the various more recent items of information into the original tetrahedral water net postulated by Hendricks.

Averaged over three cells, the lower ranges of Mg^{2+} exchange determinations afford two divalent exchange ions per three cells. These are conveniently arranged in a face-centered array on a 16×9.2 Å surface. If, then, the two open hexagonal Hendricks nets are displaced relatively along a, one-third of the " square " sections furnish four members of coordination polyhedra

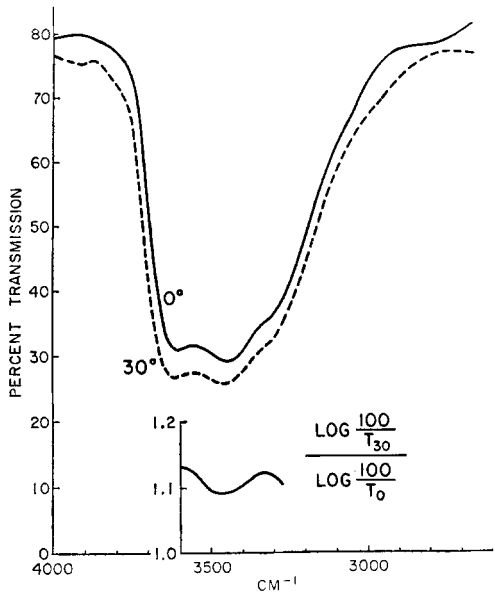

Figure 5.—Infrared absorption spectra of a flake of hydrobiotite (near two-thirds biotite, one-third vermiculite) at normal and at 30° to normal incidence (no previous heat treatment). The auxiliary curve of ratios of logs $100/T$ indicates frequencies near 3600 and 3350 cm^{-1} at which absorption increased at greater rate than the path length. Increase near 3450 is at the approximate rate of increase of the path length.

about each Mg^{2+}, and space is available for two additional water molecules to complete octahedra at each Mg^{2+} site. Tetrahedral environment is roughly maintained about each water molecule in the little-modified water net and reasonable water orientation in the octahedra articulates with it and provides protons for bonding to the silicate nets above and below, arranged and spaced as in the chlorite structure. The water molecules appear in the scheme in four different environments, but from the standpoint of any given water molecule, its own two protons either are both supplied to long bonds in the plane, or one is supplied to a short bond inclined to the plane, with the other

under a lesser influence. Of the second kind, four molecules have no one specific additional close neighbor and are probably free in inclined directions. At any rate, it seems probable that three ranges of frequencies would be absorbed in the infrared, the highest and the lowest with increasing efficiency at inclined incidences.

Actual Mg^{2+} ion populations and layer charges inferred from analyses range upward to one ion or two charges per cell. More frequent introductions of $Mg^{2+} \cdot 2H_2O$ features into the "average" model leads to a second arrangement which is easily drawn as ordered over a single cell when the

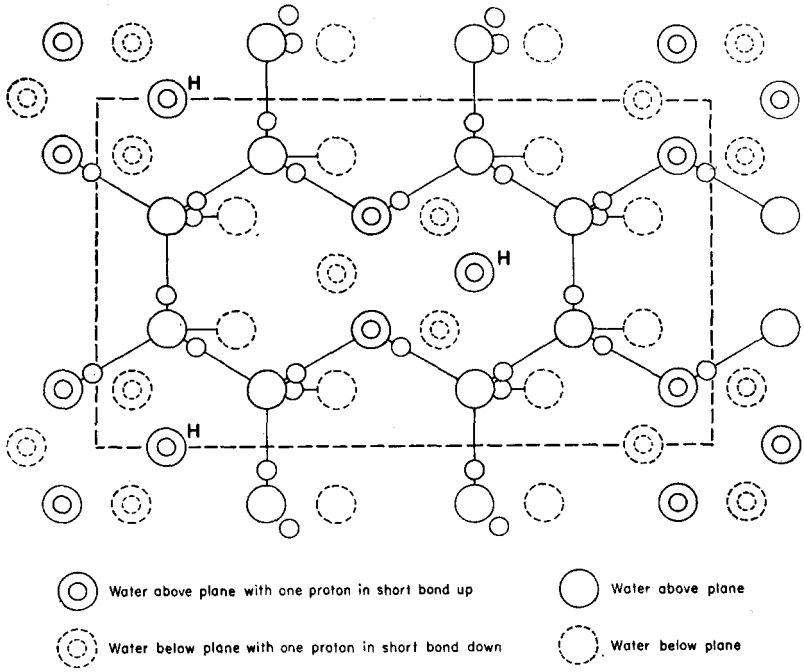

FIGURE 6.—An arrangement of interlayer water consistent with analytical information on vermiculite. A 16 × 9.2 Å section contains two octahedra of water molecules, coordinated about two Mg^{2+} exchange ions. Open hexagonal nets as postulated by Hendricks and Jefferson (1938) envelop the filled octahedra. O–H · · · · O bonds involving only water are shown as filled lines, with protons indicated along these lines for the upper water layer only. Four water molecules furnish both their protons to 3.0 Å hydrogen bonds in the plane and eight furnish one proton to a long bond and one to a short. Two molecules have no specific second neighbor.

frequency of octahedra becomes equal to the remaining open squares. Fig. 7 illustrates the two-charge capacity, and shows that the same categories of water molecules persist, only the proportions changing. Order implied in Figs. 6 and 7 is merely a convenience for drawing. It seems unlikely that orderly arrays extend through any whole crystal.

The empirical formula describing the assumptions made in Table 1 is $(Si_{8-x}\ Al_x)\ (Al_y\ Fe_z^{3+}\ Mg_{6-y-z})Mg^{2+}\ (x-y)/2\ (OH)_{4-z}\ O_{20+z} \cdot (8+x-y)H_2O$ where $(x-y) = 1.33$ and 2.00, respectively in Figs. 6 and 7. In Table 1 $(x-y)$ values are, respectively, 1.56, 1.50, 1.94 and 2.03.

The low level of agreement between observed and model exchange capacities in the Mathieson and Walker crystal is considered to be of no consequence. It arises entirely from the assumption that ferric iron did not contribute to internal charge compensation. The thought behind the assumption is that iron which oxidized after establishment of a neutral solid is easiest

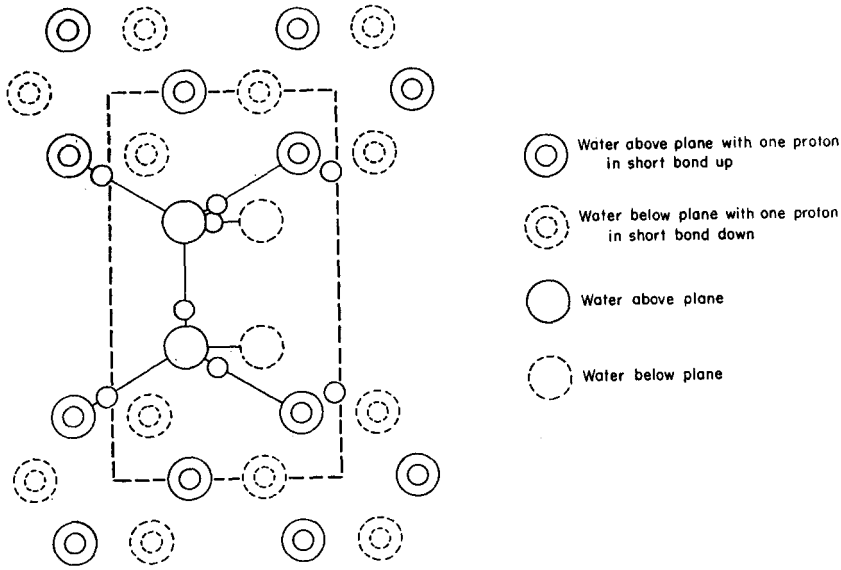

FIGURE 7.—The presumed limiting level for insertion of exchangeable Mg^{2+} ions in octahedral environment into water nets between layers charged as in the micas. Situation of hydrogen bonds within one cell for the upper water layer is indicated.

compensated by proton loss. Some ferric iron could very well have been present in the first established solid, and it is entirely possible that their exchange capacity determination did not in fact collect all the inherent exchange capacity. Agreement is satisfactory for the Grudemo analysis, in which partition of ferrous and ferric iron was made in an analysis apparently contemporary with his diffraction work, and for the Llano specimen, which was substantially iron free. To introduce the iron complication into the empirical formula quoted above, it is necessary only to partition z into z_1 (original oxidized) and z_2 (solid state oxidized), such that $z = z_1 + z_2$, the number of divalent exchange ions $= (x - y - z_1)/2$, $(OH) = 4 - z_2$, and the $H_2O = 8 + x - y - z_1$.

https://doi.org/10.1346/CCMN.1958.0070116 Published online by Cambridge University Press

REFERENCES

Barshad, Isaac, (1948) Vermiculite and its relation to biotite as revealed by base exchange reactions, x-ray analyses, differential thermal curves, and water content: *Amer. Min.*, v. 33, pp. 655–678.

Bradley, W. F., Rowland, R. A., Weiss, E. J. and Weaver, C. E. (1958) Temperature stabilities of montmorillonite- and vermiculite-glycol complexes : in *Clays and Clay Minerals*, Natl. Acad. Sci.—Natl. Res. Council, pub. 566, pp. 348–355.

Brindley, G. W. and Youell, R. F. (1953) Ferrous chamosite and ferric chamosite : *Min. Mag.*, v. 30, pp. 57–70.

Grudemo, A. (1954) x-Ray examination of the structure of vermiculite : *Swedish Cement and Concrete Res. Inst. Proc.*, no. 22, 56 pp.

Gruner, J. W. (1934) The structures of vermiculites and their collapse by dehydration : *Amer. Min.*, v. 19, pp. 557–575.

Hendricks, S. B. and Jefferson, M. E. (1938) Crystal structure of vermiculites and mixed vermiculite–chlorites : *Amer. Min.*, v. 23, pp. 851–862.

Mathieson, A. McL. and Walker, G. F. (1954) Crystal structure of magnesium-vermiculite : *Amer. Min.*, v. 39, pp. 231–255.

Serratosa, J. M. and Bradley, W. F. (1958) Determination of the orientation of OH bond axes in layer silicates by infrared absorption : *J. Phys. Chem.*, v. 62, pp. 1164–1167.

Weaver, C. E. (1958) The effects and geologic significance of potassium " fixation " by expandable clay minerals derived from muscovite, biotite, chlorite, and volcanic material : *Amer. Min.*, v. 43, pp. 839–861.